Available online at www.sciencedirect.com
SCIENCE DIRECT
Journal of Crystal Growth 287 (2006) 550–553
JOURNAL OF CRYSTAL GROWTH
www.elsevier.com/locate/jcrysgro

MOCVD growth of highly strained 1.3 μm InGaAs:Sb/GaAs vertical cavity surface emitting laser

Y.A. Chang[a,*], J.T. Chu[a], C.T. Ko[a], H.C. Kuo[a], C.F. Lin[b], S.C. Wang[a]

[a] Institute of Electro-Optical Engineering, National Chiao-Tung University, 1001 Ta-Hsieh Rd, Hsin-Tsu, Taiwan, ROC
[b] Department of Material Science and Engineering, National Chung-Hsing University, 250 Kuo-Kuang Rd, Tai-Chung, Taiwan, ROC

Available online 28 November 2005

Abstract

$In_{0.45}Ga_{0.55}As$:Sb/GaAs (1.3 μm) vertical cavity surface emitting lasers (VCSELs) were grown by metalorganic chemical vapor deposition (MOCVD). A $In_{0.45}Ga_{0.55}As$:Sb/GaAs quantum well (QW) exhibited an emission wavelength of 1.26 μm with narrow full-width at half-maximum (FWHM) of 35.9 meV. For the fabricated VCSEL with 5 μm diameter oxide-confined aperture, a room-temperature (RT) threshold current of 2.1 mA and an output power of 0.9 mW with 1.3 μm emission were obtained. The 3 dB modulation frequency was measured to be 7.6 GHz.
© 2005 Elsevier B.V. All rights reserved.

PACS: 45.55.Px; 81.15.Gh; 78.55.Cr

Keywords: A3. Metalorganic chemical vapor deposition; B1. InGaAs:Sb; B2. Semiconductor; B3. Laser diodes; B3. Optical fiber devices; B3. VCSELs

1. Introduction

Semiconductor material with emission wavelength range 1.3–1.55 μm is required for potential applications in infrared lasers, integrated optoelectronic and local-area-network systems. Long-wavelength vertical cavity surface emitting lasers (VCSELs) are key devices in the optical fiber metropolitan-area networks (MAN) [1]. To date, the most promising results on low-cost long-wavelength lasers or VCSELs have been obtained using InGaAsN quantum wells (QWs) grown on GaAs substrates [2–5]. The large conduction band offset leads to the improvement of temperature performance compared to conventional InP-based materials. The GaAs system can provide high-performance AlGaAs/GaAs distributed Bragg reflector (DBR) mirrors and allows the use of well-established oxide-confined GaAs-based VCSEL manufacturing infrastructure. However, the incorporation of N beyond about 1% into InGaAs QWs has also been found to cause strong quenching of the luminescence and broaden the luminescence. While postgrowth rapid thermal annealing can enhance the photoluminescence (PL) intensity by a factor of 10–100, a blueshift of the PL peak is found simultaneously [6,7].

InGaAs/GaAs QW structure has received much attention as a potential candidate in semiconductor laser due to its relatively uncomplicated and mature techniques. Recently, highly strained InGaAs VCSELs with PL peak at 1.205 μm and laser emission wavelength around 1.26–1.27 μm have demonstrated very promising performance and continuous-wave (CW) operation up to 120 °C as well as 10 Gb/s operation [8]. Previously, the Sb surfactant-mediated growth had been investigated in group-IV Si/SiC superlattices, and for group III–V heterostructure materials. This technology had also been utilized in InGaP bandgap control, and during the lateral epitaxial overgrowth of GaN to alter the predominant facet formation [9–11]. More recently, Sb has been shown to be an efficient surfactant, serving as an isoelectronic impurity, to provide the delay of lateral relaxation of the highly strained InGaAs QW. The Sb-assisted growth of

*Corresponding author. Tel.: +886 3 5712121x56327; fax: +886 3 5716631.
E-mail addresses: rayman0313.eo92g@nctu.edu.tw (Y.A. Chang), hckuo@faculty.nctu.edu.tw (H.C. Kuo).

0022-0248/$ - see front matter © 2005 Elsevier B.V. All rights reserved.
doi:10.1016/j.jcrysgro.2005.10.030

InGaAs has demonstrated a spectral full-width at half-maximum (FWHM) of 30 meV with PL emission at 1.19 μm [12]. A PL emission of 1.27 μm was also achieved by a 9-nm-thick $In_{0.41}Ga_{0.59}As_{0.992}Sb_{0.008}$ QW [13]. However, the PL characteristics of the Sb-assisted InGaAs QW structure with emission wavelength above 1.25 μm still need to be improved. In this study, the crystalline quality of $In_{0.45}Ga_{0.55}As$:Sb/GaAs QW active region is optimized and investigated by temperature-dependent PL. With the aim of extending the PL emission wavelength and narrowing the FWHM value, an indium-graded intermediate layer is inserted on both sides of the $In_{0.45}Ga_{0.55}As$:Sb/GaAs QW active region. Finally, a 1.3 μm $In_{0.45}Ga_{0.55}As$:Sb/GaAs double quantum well (DQW) VCSEL is fabricated and found to provide better laser performance.

2. Experiments

All structures were grown on n-type GaAs (1 0 0) substrates by low-pressure metalorganic chemical vapor deposition (MOCVD). AsH_3 and PH_3 hydride sources were used as group-V precursors. Trimethyl alkyls of gallium (Ga), aluminum (Al), indium (In) and Antimony (Sb) were the group-III precursors. The epitaxial structure was formed by an n^+-GaAs buffer, a 40.5-pair n^+-$Al_{0.9}Ga_{0.1}As/n^+$-GaAs (Si-doped) DBR, undoped active region, a p-$Al_{0.98}Ga_{0.02}As$ oxidation layer, a 25-pair p^+-$Al_{0.9}Ga_{0.1}As/p^+$-GaAs DBR (carbon-doped) and a p^+-GaAs (carbon-doped) contact layer. The graded-index separate confinement heterostructure (GRINSCH) active region mainly consisted of a DQW active region $In_{0.45}Ga_{0.55}As$:Sb/GaAs/$GaAs_{0.85}P_{0.15}$ embedded between two linear-graded $Al_xGa_{1-x}As$ ($x = 0$–0.6) confinement layers. The AsH_3/III ratio was as low as 20 and Sb/V ratio was 0.005. The thickness of the cavity active region was one wavelength. Carbon was used as the p-type dopant in the DBR to obtain higher carrier concentration (2–$3 \times 10^{18}\,cm^{-3}$). The interfaces of both the p-type and n-type $Al_{0.9}Ga_{0.1}As$/GaAs DBR layers were linearly graded to reduce the series resistance. The optical properties of QWs were optimized through PL measurement and structural analysis, as described below. The Fabry–Periot dip wavelength was determined by reflection measurement.

To realize a 1.3 μm $In_{0.45}Ga_{0.55}As$:Sb/GaAs VCSEL with better output characteristics, the QW active region is undoubtedly required to be optimized. However, the higher In content InGaAs QW, leading to the degradation of crystal quality, has been found to possess poorer optical characteristics. To extend the emission wavelength and obtain better crystalline quality, we insert an indium-graded intermediate layer on both sides of the $In_{0.45}Ga_{0.55}As$:Sb/GaAs QW. A schematic plot of the $In_{0.45}Ga_{0.55}As$:Sb/GaAs single QW grown by inserting the 2.5-nm-thick indium-graded intermediate layers is shown in Fig. 1. The indium composition in the intermediate layer on top of the QW is graded from 0.45 to 0 and with the opposite grading below the QW. The full layer thickness of the $In_{0.45}Ga_{0.55}As$:Sb QW is 10 nm. The Sb composition in $In_{0.45}Ga_{0.55}As$:Sb is 0.5%, which is determined by secondary ion mass spectroscopy (SIMS). The growth rate is about 0.5 nm/s and the growth temperature is 500 °C. Other growth conditions are similar to our prior work [14]. The thickness of the simple $In_{0.45}Ga_{0.55}As$ QW is 7 nm and the thickness of the GaAs barrier for both structures is 10 nm.

Fig. 2 shows the room-temperature (RT) PL spectra of the $In_{0.45}Ga_{0.55}As$ and indium-graded $In_{0.45}Ga_{0.55}As$:Sb single QWs. The low-PL peak intensity and the broadened FWHM of the high In content $In_{0.45}Ga_{0.55}As$ QW may be attributed to the degraded crystalline quality. Nevertheless,

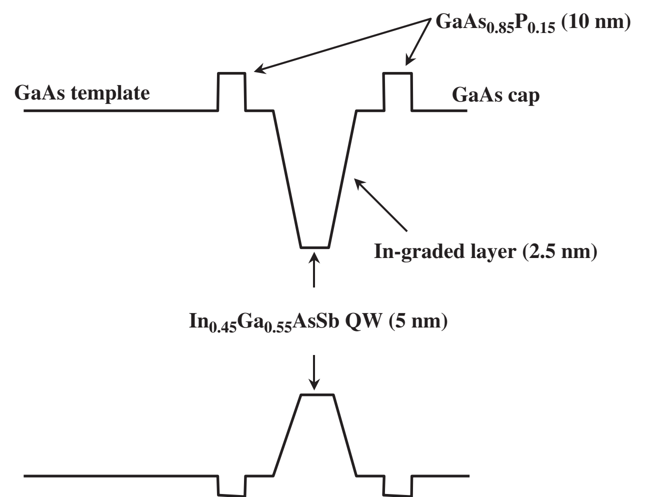

Fig. 1. A schematic plot of the $In_{0.45}Ga_{0.55}As$:Sb/GaAs single QW grown with trapezoid-potential structure by inserting the 2.5-nm-thick indium-graded intermediate layers.

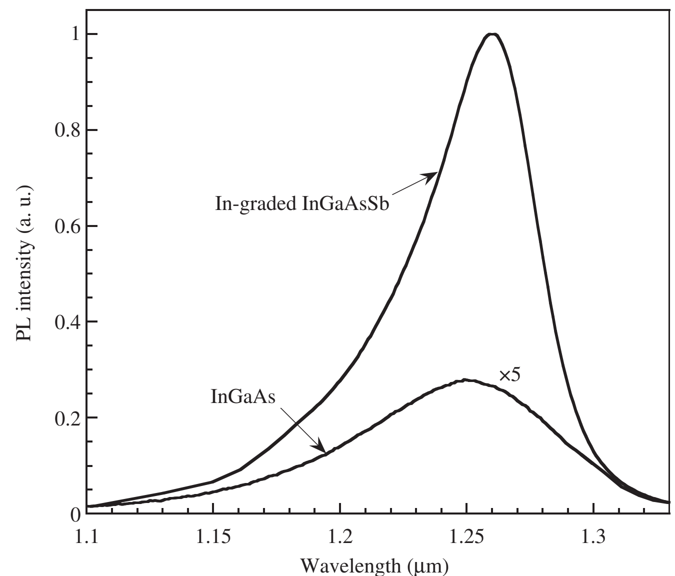

Fig. 2. RT PL spectra of the $In_{0.45}Ga_{0.55}As$ and indium-graded $In_{0.45}Ga_{0.55}As$:Sb single QWs.

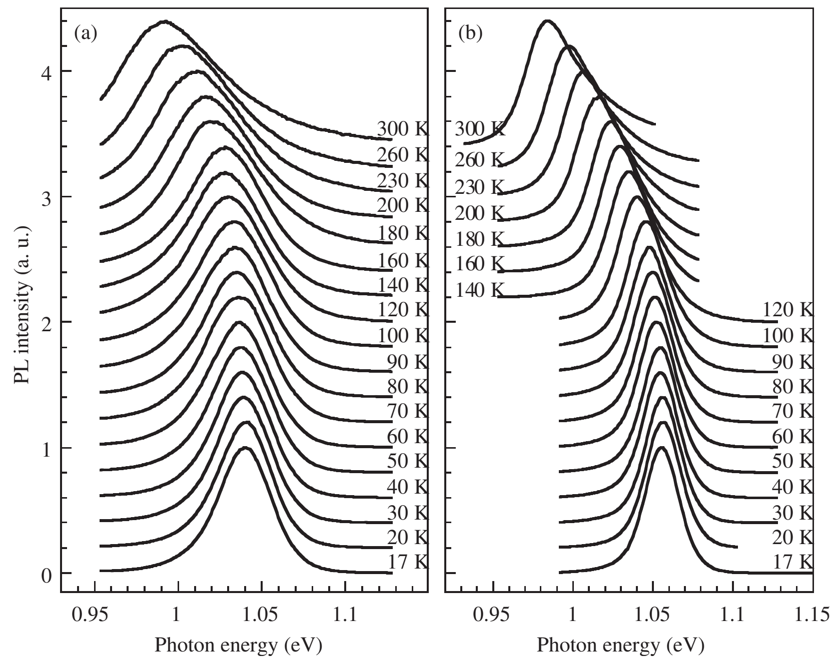

Fig. 3. Variable temperature spectra for: (a) $In_{0.45}Ga_{0.55}As$ and (b) indium-graded $In_{0.45}Ga_{0.55}As$:Sb single-QW structures.

the PL characteristics of the InGaAs/GaAs QW are improved with the assistance of Sb and the use of the indium-graded intermediate layers. An increased peak intensity factor of 20 is found with the help of Sb and indium-graded intermediate layers, while a reduction of FWHM value from 60.4 to 35.9 meV is observed. It needs to be mentioned that the PL characteristics are only slightly enhanced when the InGaAs/GaAs QW is with the indium-graded intermediate layers and without the Sb surfactant.

Variable temperature spectra for the $In_{0.45}Ga_{0.55}As$ and indium-graded $In_{0.45}Ga_{0.55}As$:Sb single-QW structures are shown in Figs. 3a and b, respectively. Smooth Gaussian peaks with strong luminescence are observed for both structures. For Sb-assisted indium-graded $In_{0.45}Ga_{0.55}As$ QW structure, the peaks are sharper, while the peak emission wavelength and the corresponding FWHM value change from 1.055 to 0.984 eV and 23.9 to 35.9 meV when the temperature is increased from 17 to 300 K. Thus, the quality of the Sb-assisted indium-graded $In_{0.45}Ga_{0.55}As$ single QW is considered to be excellent, and is suitable for the fabrication of 1.3 μm VCSEL. After fitting the experimental data to the Varshni semiempirical relationship, the bandgap energy at 0 K, α and β coefficients are 1.039 eV, $4.4\pm0.7\times10^{-4}$ eV/K and 547 ± 121 K for the $In_{0.45}Ga_{0.55}As$, and 1.054 eV, $6.3\pm1.1\times10^{-4}$ eV/K and 485 ± 124 K for the Sb-assisted indium-graded single-QW structure, respectively. Fitting our data to the classical Arrhenius law $I = I_0/\{1 + c\,\exp(-E_a/KT)\}$, according to the thermal carrier transfer mechanism, the activation energies (E_a) of our simple and Sb-assisted indium-graded $In_{0.45}Ga_{0.55}As$ single-QW structures are 20.87 and 27.09 meV, respectively.

3. Device characteristics

The processing sequence began with the deposition of a 1.3-μm-thick SiN_x layer, which acted as a hard mask in the following process, onto the wafer by plasma enhanced chemical vapor deposition (PECVD) at 300 °C. Standard photolithography and reactive ion etching (RIE) using SF_6 with a flow rate of 20 sccm as etching gas were then performed to define the etching pattern on the hard mask. The mesa diameter was 22 μm and the oxide aperture was 7 μm. After oxidation, the residual dielectric was removed, and a second 150-nm-thick SiO_2 by PECVD was deposited for passivation, followed by a partial etching process for contact window. Ti (30 nm)/Pt (50 nm)/Au (200 nm) were deposited onto the heavily p-doped GaAs contact layer for p-contact, and AuGe (50 nm)/Ni (20 nm)/Au (350 nm) were deposited for n-contact. Multiple proton implantations with a dose of $10^{15}\,cm^{-2}$ and four different proton energies between 300 and 420 keV were adopted according to simulation results of the stopping and range of ions in matter (TRIM). The implantation region was kept apart the mesa to prevent the damage which was caused by ion bombardment from destroying the active region.

The direct-current characteristic of the completed VCSEL was measured using a probe station, an Agilent 4145A semiconductor parameter analyzer and an InGaAs photodiode. The spectrum of the $In_{0.45}Ga_{0.55}As$:Sb/GaAs VCSEL was measured using an Advantest Q8381A optical spectrum analyzer. Fig. 4 plots the RT light output and voltage versus current (*L–I–V*) characteristics of the $In_{0.45}Ga_{0.55}As$:Sb/GaAs VCSEL. The RT lasing mode spectrum is shown in the inset. The VCSEL exhibits single transverse mode characteristic at a lasing wavelength of

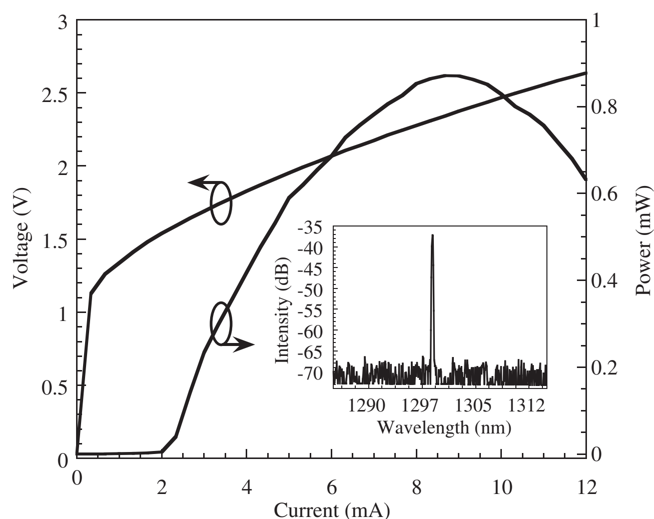

Fig. 4. RT light output and voltage versus current (*L–I–V*) characteristics of the $In_{0.45}Ga_{0.55}As$:Sb/GaAs VCSEL.

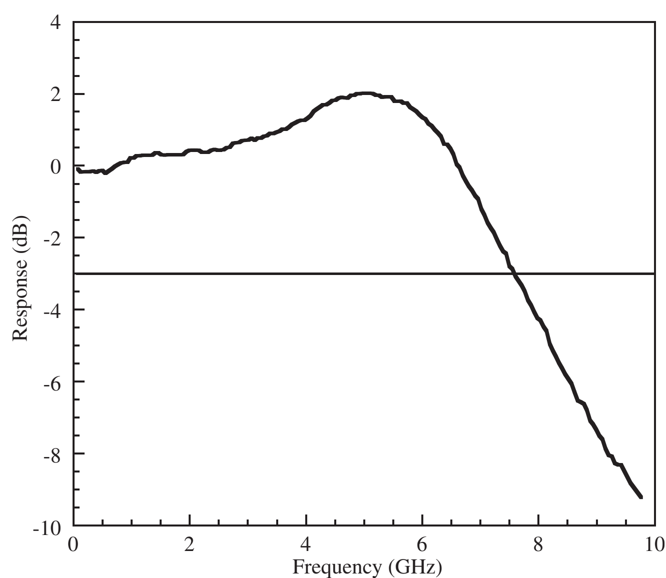

Fig. 5. Three-decibel bandwidth as a function of the biased current of the $In_{0.45}Ga_{0.55}As$:Sb/GaAs VCSEL.

1.3 μm, with a side mode suppression ratio (SMSR) of >30 dB. The maximum single mode output power exceeds 0.9 mW with a slope efficiency of 0.15 W/A at RT and the threshold current is about 2 mA. The series resistance of the VCSEL is 116 Ω.

The small signal response of VCSELs as a function of bias current was measured using a calibrated vector network analyzer (Agilent 8720) with wafer probing and a 50 μm multimode optical fiber connected to a New Focus 25 GHz photodetector. Fig. 5 plots the 3-dB bandwidth as a function of the bias current. At a bias current of 7.6 mA, the maximum 3-dB modulation frequency is measured as 7.6 GHz, which is suitable for 10 Gb/s operation.

4. Conclusion

A high-performance $In_{0.45}Ga_{0.55}As$:Sb/GaAs VCSEL was successfully grown by MOCVD. The VCSEL shows a low threshold current of 2 mA with 1.3 μm emission and a maximum output power of 0.9 mW with 0.15 W/A slope efficiency was obtained. The maximum 3-dB modulation frequency is measured as 7.6 GHz. The results of $In_{0.45}$-$Ga_{0.55}As$:Sb VCSELs can reach a performance level comparable to GaInAsN VCSELs with better thermal stability and should be considered as a very promising candidate for 1.3 μm commercial applications.

Acknowledgments

The authors would like to thank Prof. Nelson Tansu of Leigh University, Dr. Chih Ping Kuo of LuxNet Corporation, and Drs. C.P. Sung and Jim Chi of ITRI for useful discussion and technical support. This work is supported by the National Science Council, Republic of China, under grant NSC-93-2120-M009-006 and by the Academic Excellence Program of the Ministry of Education of ROC under the contract NSC-93-2752-E009-008.

References

[1] C.W. Tu, J. Phys.: Condens. Matter 13 (2001) 7169.
[2] M. Kondow, T. Kitatani, S. Nakatsuka, M.C. Larson, K. Nakahara, Y. Yazawa, M. Okai, K. Uomi, IEEE J. Sel. Top. Quantum Electron. 3 (1997) 719.
[3] K.D. Choquette, J.F. Klem, A.J. Fischer, O. Blum, A.A. Allerman, I.J. Fritz, S.R. Kurtz, W.G. Breiland, R. Sieg, K.M. Geib, J.W. Scott, R.L. Naone, Electron. Lett. 36 (2000) 1388.
[4] T. Takeuchi, Y.-L. Chang, M. Leary, A. Tandon, H.-C. Luan, D. Bour, S. Corzine, R. Twist, M. Tan, Electron. Lett. 38 (2002) 1438.
[5] M. Kawaguchi, T. Miyamoto, E. Gouardes, D. Schlenker, T. Kondo, F. Koyama, K. Iga, Jpn. J. Appl. Phys. 40 (2001) L744.
[6] A. Kaschner, T. Lüttgert, H. Born, A. Hoffmann, A.Y. Egorov, H. Richert, Appl. Phys. Lett. 78 (2001) 1931.
[7] S. Shirakata, M. Kondow, T. Kitatani, Appl. Phys. Lett. 80 (2002) 2087.
[8] P. Sundgren, R.M. von Wurtemberg, J. Berggren, M. Hammar, M. Ghisoni, V. Oscarsson, E. Odling, J. Malmquist, Electron. Lett. 39 (2003) 1128.
[9] P.O. Pettersson, C.C. Ahn, T.C. McGill, E.T. Croke, A.T. Hunter, Appl. Phys. Lett. 67 (1995) 2350.
[10] J.K. Shurtleff, R.-T. Lee, C.M. Fetzer, G.B. Stringfellow, Appl. Phys. Lett. 75 (1999) 1914.
[11] L. Zhang, H.-F. Tang, T.-F. Kuech, Appl. Phys. Lett. 79 (2001) 3059.
[12] T. Kageyama, T. Miyamoto, M. Ohta, T. Matsuura, Y. Matsui, T. Furuhata, F. Koyama, J. Appl. Phys. 96 (2004) 44.
[13] J.C. Harmand, L.H. Li, G. Patriarche, L. Travers, Appl. Phys. Lett. 84 (2004) 3981.
[14] H.-C. Kuo, H.-H. Yao, Y.-S. Chang, Y.-A. Chang, M.-Y. Tsai, J. Hsieh, E.-Y. Chang, S.-C. Wang, J. Crystal Growth 272 (2004) 538.